Self-Titrating Anticoagulant Nanocomplexes That Restore Homeostatic Regulation of the Coagulation Cascade
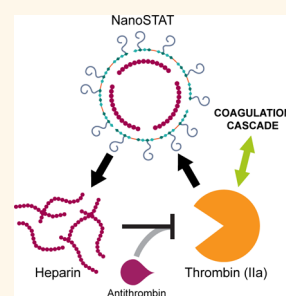
Kevin Y. Lin,[†] Justin H. Lo,[‡,§] Nikita Consul,[†] Gabriel A. Kwong,[‡] and Sangeeta N. Bhatia[‡,∥,⊥,#,⊗,*]

[†]Department of Chemical Engineering and [‡]Harvard-MIT Division of Health Sciences and Technology, Massachusetts Institute of Technology, Cambridge, Massachusetts 02139, United States, [§]Medical Scientist Training Program, Harvard Medical School, Boston, Massachusetts 02115, United States, [∥]Broad Institute of Harvard and MIT, Cambridge, Massachusetts 02142, United States, [⊥]Department of Medicine, Brigham and Women's Hospital, Boston, Massachusetts 02115, United States, [#]Electrical Engineering and Computer Science, David H. Koch Institute for Integrative Cancer Research, MIT, Cambridge, Massachusetts 02139, United States, and [⊗]Howard Hughes Medical Institute, Chevy Chase, Maryland 20815, United States

ABSTRACT Antithrombotic therapy is a critical portion of the treatment regime for a number of life-threatening conditions, including cardiovascular disease, stroke, and cancer; yet, proper clinical management of anticoagulation remains a challenge because existing agents increase the propensity for bleeding in patients. Here, we describe the development of a bioresponsive peptide—polysaccharide nanocomplex that utilizes a negative feedback mechanism to self-titrate the release of anticoagulant in response to varying levels of coagulation activity. This nanoscale self-titrating activatable therapeutic, or nanoSTAT, consists of a cationic thrombin-cleavable peptide and heparin, an anionic polysaccharide and widely used clinical anticoagulant. Under nonthrombotic conditions, nanoSTATs circulate inactively, neither releasing anticoagulant nor significantly prolonging bleeding time. However, in response to life-threatening pulmonary embolism, nanoSTATs locally release their drug payload and prevent thrombosis. This autonomous negative feedback regulator may improve antithrombotic therapy by increasing the therapeutic window and decreasing the bleeding risk of anticoagulants.

KEYWORDS: nanomedicine · anticoagulation · protease · stimuli-responsive · self-regulation

Homeostatic regulation plays a critical role in human health and underlies diverse biological processes, including hormone release,[1] ionic balance,[2,3] and cell-mediated immunity.[4,5] In particular, living systems employ negative feedback circuits to maintain processes within physiologic limits, preventing unrestricted amplification cascades or positive feedback cycles.[6–8] A key homeostatically regulated process with significant medical relevance is blood coagulation, the protease-driven positive-feedback cascade by which clots are formed to stop blood loss from injured vessels. Dysregulation of this process, whether pathological or drug-induced, leads to adverse outcomes: insufficient coagulation promotes life-threatening hemorrhage, while uncontrolled coagulation drives thrombosis—or intravascular clotting—the potentially fatal medical condition underlying pulmonary embolism, stroke, and organ infarction.[9] Clinical prevention of thrombosis revolves around the administration of anticoagulants, the levels of which must be tightly controlled within a narrow therapeutic window to prevent coagulation and limit life-threatening bleeds that are their primary side effect.[10] Consequently, anticoagulants require strict dose titration and monitoring,[11,12] and there remains a pressing need for safe, yet effective agents to improve the treatment of thrombosis.

The advent of nanotechnology has enabled a plethora of engineering approaches for improving the efficacy and safety profiles of drugs.[13,14] A number of these nanoscale drug delivery schemes have drawn inspiration from the ability of biological systems in nature to coordinate multiple molecular components to produce emergent behaviors, in order to design nanosystems that communicate across multiple length scales, form positive feedback loops,
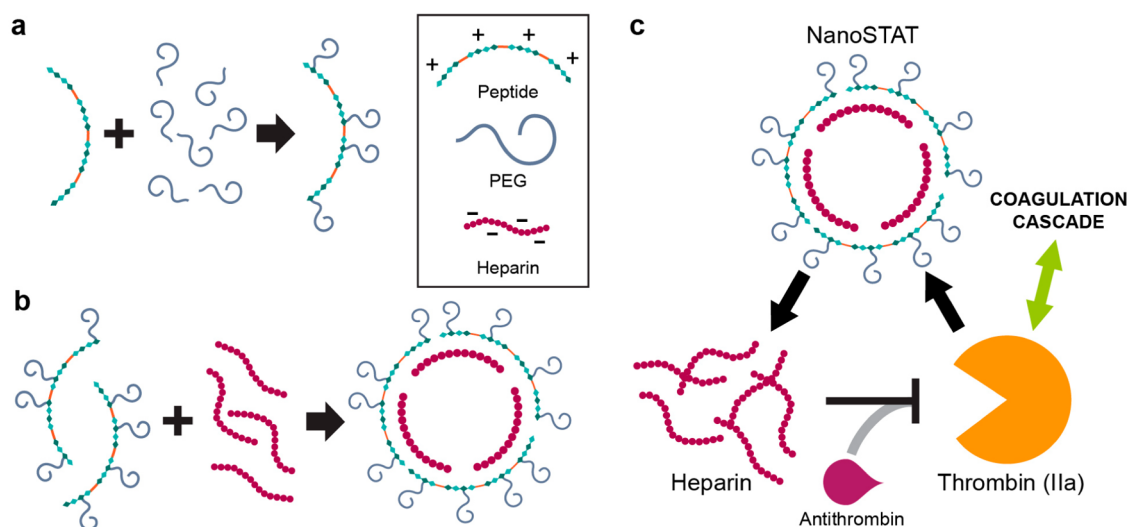
Figure 1. Schematic of self-titrating activatable therapeutic. (a) PEGylation of peptides used to form nanoSTATs. (b) Self-assembly of cationic PEG-peptide and anionic heparin to form nanoSTATs. (c) Negative feedback system for self-titrating release of heparin in response to thrombin activity.

and drive accumulation of drugs at disease sites.[15−17] Here, inspired by the human body's capacity to precisely orchestrate and control biological reaction networks, we sought to engineer nanoagents that could autonomously regulate coagulation by self-titrating the release of a systemically administered anticoagulant, thereby improving its safety profile. Existing delivery strategies for anticoagulants have explored the use of biodegradable polymers for controlled release,[18−20] multivalent presentation to increase potency,[21,22] or reformulated drugs to enable alternative routes of administration.[23] While anticoagulants have previously been packaged in nanoparticle form, these open-loop systems deliver their cargo without any form of feedback regulation and cannot autonomously titrate the release of drugs in response to dynamic circulatory conditions within the body.

In this study, we reformulate unfractionated heparin (UFH), the prototypical clinical anticoagulant,[24] into a self-assembled nanocomplex that is responsive to thrombin, a key protease of the coagulation cascade, by leveraging the charge interaction of PEGylated cationic peptides composed of thrombin-cleavable substrates (Figure 1A) with naturally anionic heparin (Figure 1B). The resultant complexes release heparin in response to thrombin activity, which then interacts with endogenous antithrombin (ATIII) to inhibit thrombin, the initial trigger of drug release, thereby creating a negative feedback control circuit (Figure 1C). This thrombin-activated release mechanism deploys more anticoagulant during thrombosis, when the generation of thrombin outpaces endogenous regulatory checkpoints, compared to healthy coagulation, which is normally tightly regulated. We explore the composition of PEGylated nanocomplexes and characterize their *in vitro* and *in vivo* release of heparin, efficacy in

a pulmonary embolism model of thrombosis, and impact on systemic bleeding time. This nanoscale self-titrating activatable therapeutic (nanoSTAT) has the potential to prevent thrombosis with fewer bleeding side effects than its free counterpart.

RESULTS

Synthesis and Characterization of NanoSTATs. Unfractionated heparin is a mainstay drug used in the hospital setting; yet, it is particularly difficult to dose due to its unpredictable pharmacokinetics. Thus, its use requires clotting time measurements and dose readjustment every 3−4 h to maintain drug levels within the therapeutic range.[25−27] Because it is highly anionic, heparin is readily sequestered by cationic peptides,[28,29] such as its clinical antidote protamine, which is characterized by a very high net positive charge.[30] Therefore, we designed a cationic peptide sequence with multiple arginine/lysine-rich regions separated by thrombin-cleavable substrates (LVPR.RK4 sequence = rkrk-(LVPRG-rkrk)₃, lower case = D-isomer) that is capable of inhibiting heparin activity while intact, yet releases active heparin following degradation by thrombin.[31] D-Amino acids were used for the nonsubstrate regions of the peptide in an effort to minimize nonspecific proteolytic degradation. To further stabilize the nanocomplexes in ionic solutions, prevent nonspecific protein interactions, prolong circulation time, and improve biodistribution, we conjugated the FDA-approved polymer poly(ethylene glycol) (PEG, 5 kDa) to a subset of the lysine residues using amine-reactive ester chemistry (Figure 1A).[32,33] When the heparin (∼18 kDa average MW) and PEG-LVPR.RK4 conjugate were mixed together, they self-assembled into spherical nanoscale complexes, or nanoSTATs, as confirmed by transmission electron microscopy (Figure 2A).
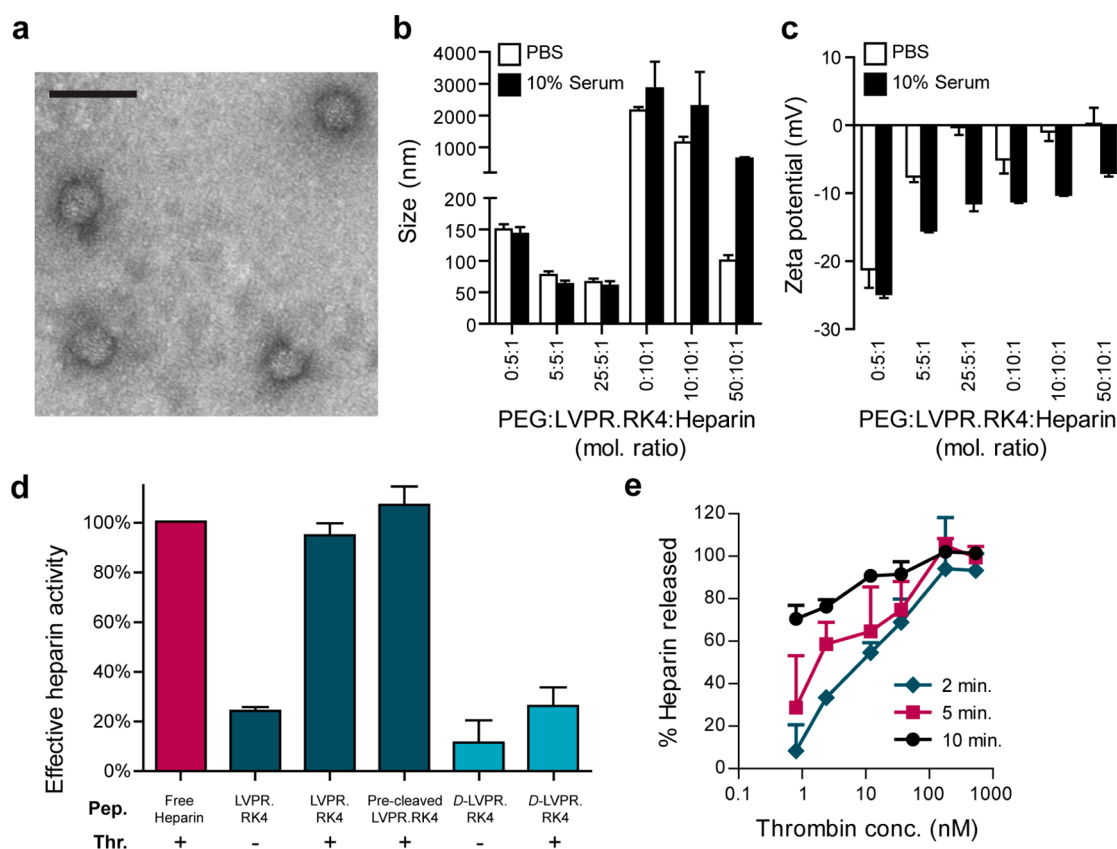
Figure 2. *In vitro* characterization of nanoSTATS. (a) Transmission electron microscopy image of negatively stained nanoSTATs with a 25:5:1 PEG:LVPR.RK4:heparin molar ratio (scale bar = 100 nm). (b) Mean hydrodynamic diameter of nanoSTATs at varying PEG:LVPR.RK4:heparin ratios in PBS and 10% serum ($n = 3$ per condition, SD). (c) Zeta potential of nanoSTATs at varying PEG:LVPR.RK4:heparin ratios in PBS and 10% serum ($n = 3$ per condition, SD). (d) Heparin activity when complexed with peptides and incubated with thrombin, as determined by anti-FXa assay ($n = 3$ per condition, SD). Pep, peptide; *D*, D-isomer; Thr, thrombin. (e) Release profile of heparin from nanoSTATs as a function of thrombin concentration and incubation time. Amount of heparin released was determined by anti-FXa assay ($n = 3$ per condition, SD).

To explore the impact of component ratios on complex formation, we tested PEG:LVPR.RK4 reaction ratios between 0:1 and 5:1 (mol/mol) and LVPR.RK4: heparin mixing ratios of either 5:1 or 10:1 (mol/mol). For each particle composition, we measured the resultant nanoSTAT particle size and zeta potential in phosphate-buffered saline (PBS) or 10% exosome-free fetal bovine serum *via* dynamic light scattering (DLS). In both solutions, increasing the LVPR.RK4:heparin mixing ratio from 5:1 to 10:1 caused the nanoSTAT hydrodynamic diameter to increase in size from the nano- (~150 nm) to the microscale (~2−3 µm), while increasing the PEG:LVPR.RK4 reaction ratio decreased the complex size (Figure 2B). The zeta potential of nanoSTATs was generally negative, particularly in 10% serum, with the addition of PEG bringing the charge closer to neutrality (Figure 2C). A component ratio of 25:5:1 PEG:LVPR.RK4:heparin generated the smallest particles (hydrodynamic diameter ~50 nm) and was used for the remainder of *in vitro* and *in vivo* experimentation. Finally, since some charged nanomaterials are known to produce cytotoxic profiles,[34,35] we incubated human endothelial cells (HUVECs) with nanoSTATs at representative therapeutic heparin

concentrations and established that no toxicity was observed up to 10 U/mL, which corresponds to a ~1000 U/kg heparin dose in the bloodstream, or an order of magnitude higher than standard dosing regimens (Figure S1).[36] Furthermore, to confirm the safety profile of nanoSTATs *in vivo*, we performed blood smear analyses and hematoxylin and eosin staining of organs at time points 1, 4, and 24 h following the intravenous administration of 25:5:1 nanoSTATs (200 U/kg heparin) in mice, the dose used hereafter in our therapeutic studies. The peripheral blood smears did not demonstrate any changes in blood cell morphology or the leukocyte differential compared to free heparin-treated or untreated controls (Figure S2), and the H&E section did not show signs of inflammation, tissue damage, or cell death (Figure S3).

Veiling and Unveiling of NanoSTATs *in Vitro*. Next, we assayed whether nanoSTATs could regulate the release of heparin in response to clotting activity. We exploited the serine protease thrombin as the drug release trigger on the basis of its critical role in catalyzing the formation of fibrin clots and regulating hemostasis through positive and negative feedback circuits and its sensitivity to inhibition by heparin.[37] To characterize

thrombin-triggered disassembly, we incubated nano-STATs with or without thrombin (500 nM) at 37 °C and assayed the samples by analytical FPLC. The control sample chromatogram exhibited a sharp peak at ~7 mL corresponding to intact nanoSTATs, which was absent in the presence of thrombin and instead replaced by a broad peak from ~11 to 17 mL, corresponding to the profile of free heparin (Figure S4); free heparin was therefore below the limit of detection in the sample of intact nanoSTATs and released upon incubation with thrombin. To confirm the essentially complete incorporation of free heparin into nano-STATs, we performed an electrophoretic gel retardation assay followed by Alcian Blue staining for heparin, showing that the free heparin band is absent from the nanoSTAT sample lane (Figure S5). To determine the accessibility of heparin when complexed, we mixed nanoSTATs with Azure II, a metachromatic dye that exhibits a shift in absorbance upon electrostatic interaction with heparin. We observed that intact nano-STATs exhibited little interaction with Azure II, while nanoSTATs incubated with thrombin (500 nM) caused a significant increase in absorbance at 530 nm (Figure S6).[23] Taken together, these data demonstrate that heparin is shielded from external charge interactions when complexed and that thrombin cleavage of the PEG-LVPR.RK4 causes the dissociation of the charge-based nanoSTATs and results in the release of heparin.

To investigate whether the complexation of heparin modulates its anticlotting activity, we performed an anti-Factor Xa (FXa) assay on samples of intact and thrombin-cleaved nanoSTATs. This assay measures heparin activity based on its capacity to inhibit the enzymatic activity of FXa, one of several serine protease targets of heparin, using a chromogenic substrate. Intact heparin-containing nanoSTATs reduced heparin activity by ~80% relative to free heparin, while heparin activity was fully restored when nanoSTATs were incubated with thrombin (Figure 2D). In light of the evidence that free heparin is nearly completely encapsulated by nanoSTAT particles (Figures S4 and S5), the residual ~20% heparin activity observed in intact nanoSTATs suggests that not all bound heparin was rendered biologically inactive, though it is possible that trace amounts of noncomplexed heparin may contribute to the residual activity. Heparin activity did not differ between preformed complexes incubated with thrombin and free heparin mixed with peptides that had been previously cleaved by thrombin, confirming that peptide cleavage sites remain accessible while embedded in nanoSTATs and that cleaved LVPR.RK4 fragments are unable to inhibit anticoagulant activity. Furthermore, incubation of nano-STATs formed with D-stereoisomers of LVPR.RK4 (which confers resistance against protease cleavage) with thrombin led to minimal unveiling of heparin activity,

supporting the interpretation that thrombin cleavage of LVPRG sites is responsible for the functional unveiling of heparin. These experiments show that our peptide−heparin nanoSTATs veil heparin activity when intact but release fully functional heparin in response to thrombin cleavage.

Coagulation is a dynamic process where as little as ~10−30 nM of activated thrombin is needed to form a fibrin clot and up to 300−1000 nM of total thrombin can be generated within minutes.[38] To investigate the kinetics of heparin release under physiologically relevant conditions, we incubated nanoSTATs with different concentrations of thrombin (1−1000 nM) and monitored heparin release following defined periods (2, 5, and 10 min) by the anti-FXa assay. As anticipated, the observed elevation in heparin release followed the track of increasing thrombin concentration, reaching a plateau of nearly complete release (>95%) in response to 180 nM thrombin for all incubation times tested (Figure 2E). Similarly, heparin release increased over time in response to thrombin exposure across the range of concentrations tested. These data indicate that heparin release is a function of thrombin activity and time at physiologically relevant concentrations and time scales, behavior that reflects the self-titrating properties of nanoSTATs.

NanoSTATs Exhibit Responsive Behavior *ex Vivo*. To test the effect of nanoSTATs on plasma, we first performed an activated partial thromboplastin time (aPTT) clotting assay, which is used clinically to monitor heparin levels in patients by measuring the time it takes a plasma sample to clot when coagulation is triggered by an activator such as silica or ellagic acid. Current clinical guidelines for heparin treatment recommend dose ranges that yield aPTTs ~1.5−2.3-fold above the control bleeding time, which yields a relatively narrow therapeutic window that is further complicated by the need for each laboratory to internally standardize and validate their own reference ranges.[12,36] In human plasma samples spiked with free heparin, the clotting time increased dramatically in a dose-dependent manner from ~29 s in the absence of heparin (0 U/mL) up to ~44 s (~1.5-fold over control) with exposure to only 0.8 U/mL and as long as ~136 s (~5-fold over control) for 2.0 U/mL (Figure 3A). In contrast, plasma samples spiked with identical doses of heparin nanoSTATs exhibited significantly shorter increases in clotting time, reaching 46 s (~1.5-fold over control) at a dose of only 2 U/mL ($p < 0.001$ by Student's *t*-test, $n = 3−4$ per condition). Our results indicate that, relative to the free form, an equivalent dose of heparin sequestered within nanoSTATs leads to a significantly shorter aPTT, which is clinically associated with lower risk of bleeding[39,40] and suggests that nanoSTATs may offer a wider therapeutic window than traditional UFH treatment.
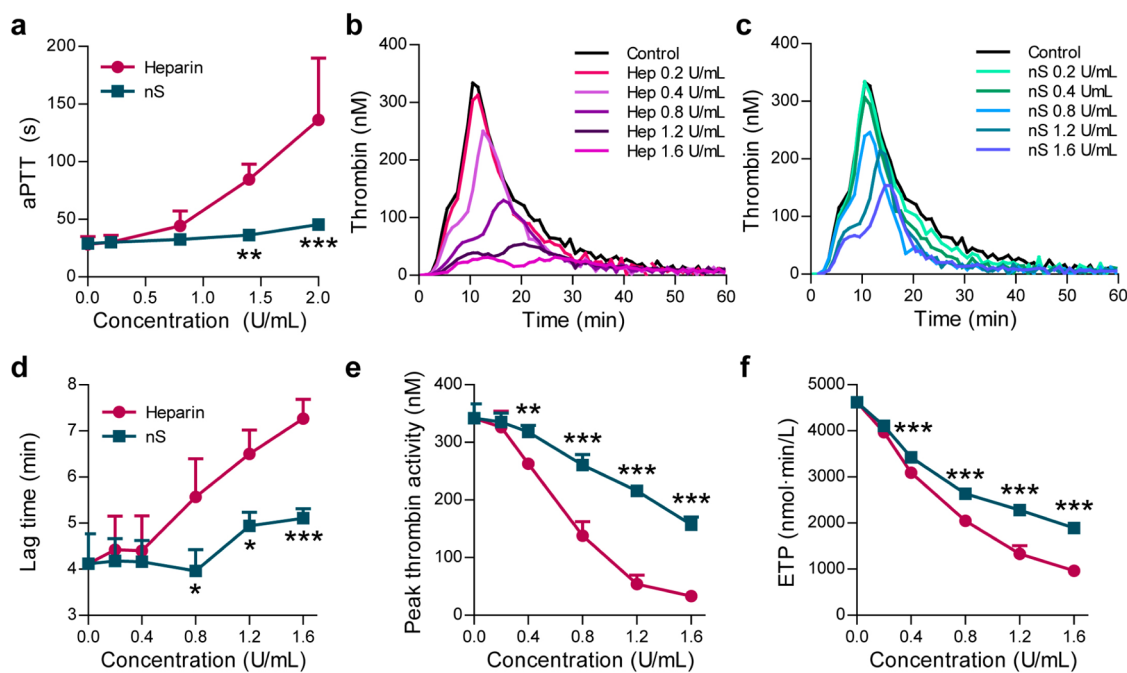
Figure 3. *Ex vivo* characterization of nanoSTATs in human plasma. **(a)** Activated partial thromboplastin time of normal human control plasma spiked with free heparin or nanoSTATs (nS) (**$p < 0.01$; ***$p < 0.001$ by two-way ANOVA with Bonferroni post test; $n = 3$ per condition, SD). **(b, c)** Real-time thrombin generation in plasma in the absence or presence of increasing concentrations of **(b)** free heparin (Hep) or **(c)** nanoSTATs ($n = 3$ per condition). **(d)** Lag time, **(e)** peak thrombin, and **(f)** endogenous thrombin potential (ETP) calculated from the thrombin generation assays in **(b)** and **(c)** (*$p < 0.05$ by two-way ANOVA with Bonferroni post test; $n = 3$ per condition, SD).

To further analyze the anticoagulant mechanism of the nanoSTATs, we performed real-time thrombin generation assays in human plasma. The thrombin generation curves of free heparin and nanoSTATs exhibited distinct patterns (Figure 3B,C, Figure S7). The time to initial thrombin formation (lag time), which correlates with clot initation, was prolonged in a dose-dependent manner by free heparin as expected. In contrast, the lag time of plasma samples with identical doses of nanoSTATs did not change markedly as the effective concentration of heparin increased (Figure 3D, $p < 0.01$ by Student's *t*-test, $n = 3$ per condition).[41,42] These results were consistent with the aPTT assay and support the model that nanoSTATs initially veil complexed heparin and block its activity. Following the onset of clotting, nanoSTATs demonstrated anticoagulant activity similarly to free heparin by reducing the maximum (peak) and total (endogenous thrombin potential, ETP) thrombin generation relative to the untreated control (0 U/mL), suggesting that the nanoSTATs release active heparin during the clotting process. However, the magnitude of the reductions in peak thrombin and ETP was significantly smaller for nanoSTATs at equivalent heparin concentrations greater than 0.2 U/mL ($p < 0.001$ by Student's *t*-test, $n = 3$ per condition; Figure 3E,F). This trend was particularly apparent in the peak thrombin activity, which shows that the generation of activated thrombin is needed to first release heparin from the nanoSTATs in order to block further coagulation, as opposed to

free heparin, which is active from the outset. The ETP of nanoSTATs never decreased below 40% of the baseline level even at the highest dose tested (1.6 U/mL), which was over twice the maximum recommended dose of UFH,[12,25,36] whereas the equivalent concentration of free heparin reduced the ETP by ~80%. This observation suggests that nanoSTATs may buffer against safety risks from dose escalation, as studies have shown that reductions in ETP greater than 80% relative to normal baseline have been correlated with risk of bleeding in patients.[43,44]

NanoSTATs Remain Veiled in the Absence of Thrombosis and Do Not Increase Bleeding. In the bloodstream, nanoSTATs must navigate a complex milieu of proteins and plasma components without experiencing premature release of their cargo until exposed to sites of thrombus formation. To validate whether anticoagulant activity of nanoSTATs remains suppressed *in vivo* under healthy conditions, we performed two sets of circulation time experiments. First, using fluorescently labeled heparin, we sampled the blood of mice injected with either nanoSTATs or free heparin (100 U/kg, $n = 3$ mice) and measured the plasma fluorescence over time (Figure 4A). These results indicated that nanoSTATs exhibited a rapid initial clearance half-life within minutes, while a secondary half-life persisted for greater than an hour, which was consistent with the clearance behavior of other heparin-functionalized nanoparticles.[45] Next, we injected mice with either nanoSTATs or free heparin and tested the plasma for
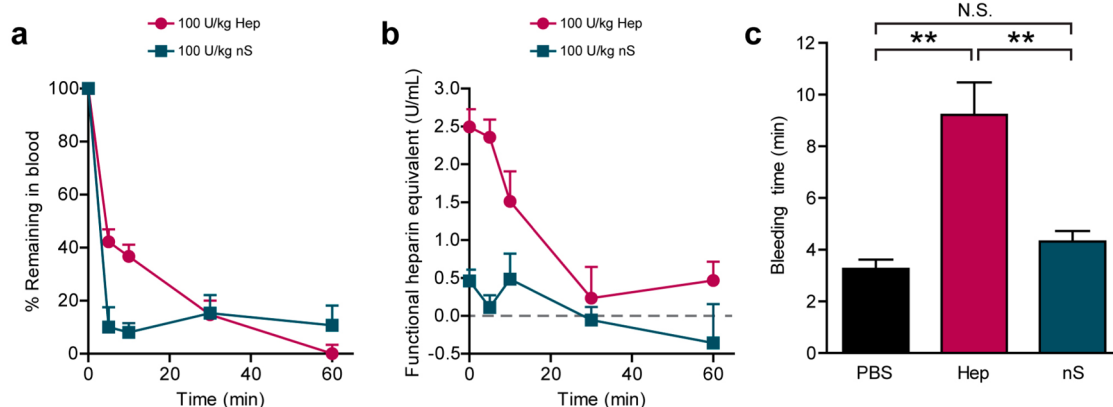
Figure 4. *In vivo* bleeding time of nanoSTATs. (a) Circulation time of nanoSTATs (nS) and free heparin as determined by fluorescence using FITC-heparin ($n = 3$ mice, SE). (b) Circulation time of nanoSTATs (nS) and free heparin (Hep) as determined by anti-FXa assay on mouse plasma samples withdrawn over time ($n = 3$ mice, SE). (c) Tail bleeding time of mice administered 200 U/kg of free heparin or nanoSTATs (**$p < 0.01$ by one-way ANOVA with Tukey post test; $n = 5-7$ mice, SE).

heparin activity using the anti-FXa assay (Figure 4B). This experiment showed that unlike the functional activity of free heparin, which matched its fluorescence signal, nanoSTATs exhibited little to no heparin activity at any of the measured time points. Together, these studies showed that nanoSTATs veil heparin function while in circulation, leading to reduced levels of heparin activity in the blood pool relative to free heparin.

The primary side effect of clinical anticoagulants, including heparin, is moderate to potentially fatal bleeding.[10,11] To assess whether nanoSTATs reduce bleeding side effects, we performed tail transections on mice after they were treated intravenously with nanoSTATs (200 U/kg), free heparin (200 U/kg), or PBS (control) and measured the time elapsed until bleeding ceased (Figure 4C). Free heparin increased the mean bleeding time of mice ($\sim$9.2 min) by greater than 280% over that of control PBS-treated mice ($\sim$3.3 min). By contrast, the mean bleeding time of nanoSTAT-treated mice ($\sim$4.3 min) was significantly shorter than that of the heparin-treated group and only 30% longer than the control bleeding time ($p < 0.01$ by one-way ANOVA with Tukey post test, $n = 5-7$ mice). The reduction in the bleeding time of mice administered with nano-STATs *versus* free heparin suggests that the level of thrombin activity in response to injury did not unveil sufficient heparin to significantly impact bleeding cessation. This finding may be due to the fact that sealing major wounds is largely dependent on platelet activation and plug formation, a process that requires considerably lower levels of activated thrombin than during thrombus formation.[46,47] Taken together, these data showed that nanoSTATs circulate in an inactive form, veiling heparin activity and decreasing the risk of bleeding.

NanoSTATs Prevent Thrombosis *in Vivo*. To evaluate the ability of nanoSTATs to prevent thrombosis *in vivo*, we utilized a thromboplastin-induced model

of pulmonary thromboembolism, which we and others have shown leads to deposition of microembolisms primarily in the lungs (Figure S8).[48,49] Mice were administered fibrinogen labeled with near-infrared dyes to monitor the formation of fibrin clots in the lungs by fluorescent imaging after thromboplastin challenge (2 μL/g b.w.). The lungs of mice treated with nanoSTATs (200 U/kg) showed a $\sim$75% reduction ($p < 0.01$, one-way ANOVA with Tukey post test, $n = 5$ mice) in the burden of clots compared to the lungs of control-treated mice (Figure 5A,B). This reduction in the formation of clots caused by nanoSTATs was statistically equivalent to the therapeutic efficacy achieved by the corresponding dosage of free heparin (200 U/kg, Figure S9). Moreover, histological analysis showed that microvessels in the lungs of control-treated animals contain thrombi (arrows in Figure 5C, top right panel), whereas such vessels in animals treated with either free heparin or nanoSTATs were largely patent, as evidenced by the presence of red blood cells (arrow heads in Figure 5C). Combined with the data from the tail bleeding assay, these observations suggest that nanoSTATs prevent thrombosis as effectively as free heparin but with a significantly reduced risk of bleeding.

DISCUSSION

Anticoagulation is vital for the prophylaxis and treatment of life-threatening thrombosis; however, inhibiting the body's natural ability to form blood clots predisposes patients to severe bleeding complications. The ideal anticoagulant is a drug that prevents coagulation without promoting bleeding.[9,11] Here, we engineered a nanocomplex that autonomously titrates the release of anticoagulant in response to endogenous levels of activated thrombin in thrombosis, creating a negative feedback circuit that regulates the coagulation cascade with negligible increases to the risk of bleeding. While Maitz *et al.* also recently
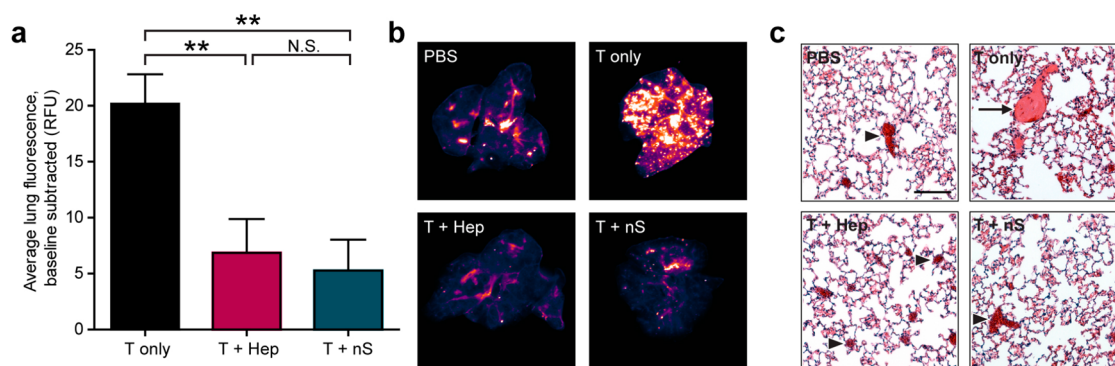
Figure 5. *In vivo* therapeutic efficacy of nanoSTATs. (a) Quantification of fibrin deposited in the lungs of mice dosed with thromboplastin (T, 2 μL/g body weight) and nanoSTATs (nS, 200 U/kg) or free heparin (Hep, 200 U/kg) (**$p < 0.01$ by one-way ANOVA with Tukey post test; $n = 5$ mice, SE). (b) Near-infrared fluorescent scans of excised lungs to assess VT750-labeled fibrinogen following intravenous injection of PBS, T only, T + nS, and T + Hep. (c) H&E staining of lungs in mice under the same conditions as in (b). Arrow denotes fibrin clots; arrowheads denote patent vessels (scale bar = 100 μm).

assessed the function of a self-regulating anticoagulant material through *ex vivo* simulations, we tested our nanoSTATs *in vivo* and demonstrated therapeutic and safety characteristics that can only be investigated in animal models. Furthermore, our nanoformulation is designed for systemic thrombosis prevention in contrast to their hydrogel platform, which is better suited for highly localized anticoagulation applications (*e.g.*, surface coating of blood contacting medical devices).[8] Engineering approaches have also been used to design bioresponsive thrombolytics—antithrombotic therapies designed to dissolve existing clots rather than prevent their formation—including recombinant proteins[47,50] or polymeric microparticles[51] activated by proteolytic or biophysical triggers associated with thrombosis that decrease bleeding and expand therapeutic windows. Looking forward, several clinical applications warrant further investigation with our nanoSTATs. Since the model used here mimics the development of emboli in the microvasculature, future testing will assess nanoSTATs' ability to treat thrombosis in larger vessels, which are representative of clinical situations such as myocardial infarction or thrombotic stroke.[52,53] Further studies are also needed to understand the impact of the nanoSTAT formulation on other side effects associated with UFH, such as heparin-induced thrombocytopenia and platelet dysfunction.[25,54,55]

Numerous recent nanoscale drug delivery systems utilize responsiveness to biological stimuli to control drug biodistribution *in vivo*.[56,57] A majority of these systems operate without the ability to self-regulate; such nanoparticles are adequate for site-directed delivery, but impractical for applications requiring adjustable functionality under varying biological conditions. Only a small number of self-regulating nanocarriers have been developed, with glucose-responsive insulin delivery being the most well-known example.[58,59] In contrast to the glucose–insulin feedback loop, which functions over several hours through the body's downstream response to insulin to indirectly affect the initial

glucose trigger,[60] we have designed a direct negative feedback loop that immediately modulates its proteolytic trigger in conjunction with a single readily available effector, an approach that is well suited for regulating enzymatic cascades that operate on rapid time scales. Our strategy was achieved through facile noncovalent modification of the clinically approved anticoagulant UFH using biocompatible materials, which may mitigate the translational risk of this nanotherapeutic. A more detailed examination of the nanoSTATs' impact on hemodynamic parameters and immunological markers would help to verify the *in vivo* safety of the system.[30] The clearance kinetics of nanoSTATs suggest they may be well-suited for administration by continuous infusion in an in-patient setting, where rapid cessation of anticoagulation is often required in order to undertake further medical procedures. For longer-term prophylactic applications, strategies for extending the circulation time of the nanoSTATs may be required, such as optimizing the density and attachment sites of PEG, using longer chain polymers, and varying the ratio of non-PEGylated to PEGylated peptides. Other potential improvements to our system include the use of alternative peptide substrates that are sensitive to upstream coagulation factors such as FXa,[61] further functionalizing nanoSTATs with fibrin-targeted ligands to concentrate drugs in areas of clotting,[17,62,63] and delivering direct coagulation inhibitors instead of UFH.[64] Furthermore, this paradigm is readily extensible to the regulation of additional disease-associated proteases *via* the modular protease-sensitive and therapeutic-binding domains, enabling the design of next-generation self-titrating medicines.

CONCLUSION

In summary, this work represents, to the best of our knowledge, the first self-titrating anticoagulant nanoformulation that decreases the risk of bleeding while maintaining antithrombotic efficacy. By incorporating

negative feedback control, nanoSTATs further expand the repertoire of nanomedicines available for the treatment of thrombosis and may lead to the development of safer antithrombotics.

MATERIALS AND METHODS

Peptide Synthesis and Functionalization. Peptides (LVPR.RK4 = rkrkLVPRGrkrkLVPRGrkrkLVPRGrkrk, lower case = D-isomer) were synthesized by standard FMOC solid-phase peptide synthesis (Koch Institute Biopolymers Core or Tufts University Core Facility), lyophilized, and resuspended at 5 mg/mL in ddH$_2$O. Peptides were PEGylated through incubation of a 5 mg/mL stock peptide solution with amine-reactive 5000 Da poly-(ethylene glycol)-succinimidyl valerate (PEG-SVA, Laysan Bio Inc.) for 1 h at room temperature.

Physical Characterization of NanoSTATs. NanoSTATs were generated with peptide and PEG molar ratios as reported, with a fixed heparin (sodium salt from porcine mucosa, Sigma, ~18 000 Da average MW) concentration of 20 U/mL (~0.1 mg/mL) unless reported otherwise. For measurements in ionic solutions, 10× PBS stock was added to preformed nanoSTAT solutions for a final concentration of 1× PBS. For measurements in serum, bovine serum (Gibco) was added to a concentration of 10% (v/v). Mean hydrodynamic diameter was determined via dynamic light scattering of a 50 μL sample at 20 U/mL heparin (ZetaSizer Nano Series, Malvern). Zeta potential was measured via electrophoretic light scattering on a 900 μL particle sample at 20 U/mL (ZetaSizer Nano Series). The morphology of nano-STATs was visualized by dialyzing overnight against 1× PBS in 20 kDa MWCO dialysis cassettes (Thermo), negatively staining samples with 2% uranyl acetate, and imaging via transmission electron microscopy using an FEI Tecnai Spirit operated at 80 kV.

Veiling and Unveiling of Function in Vitro. The heparin activity of intact nanoSTATs was determined using the anti-FXa assay (Sekisui Diagnostics) according to manufacturer instructions. The release of heparin was determined by incubating nanoSTATs with various concentrations of human thrombin (Haematologic Technologies) at 37 °C for the reported amounts of time. The activity of the released heparin was then determined using the anti-FXa assay.

Cytotoxicity Assays. Human umbilical vein endothelial cells (passage 9) were cultured in EGM-2 media (Lonza) on a 96-well plate. When cells reached 70% confluency, nanoSTATs, PEG-LVPR.RK4, free LVPR.RK4, or free heparin was added as a 9× stock in PBS, diluted in EGM-2. After 24 h elapsed, cell viability was quantified by the MTS assay (CellTiter AQueous One, Promega) based on OD490 after 1 h incubation.

Blood Smears. Swiss Webster mice were injected with nano-STATs or free heparin at 200 U/kg body weight. Blood was sampled at the specified time points by retro-orbital collection with uncoated capillaries (Drummond), mixed with 1× PBS with 10 mM EDTA, and spread onto glass slides using standard preparation techniques. Dried blood smears (3 smears per time point) were stained with Wright-Giemsa stain in methanol (Sigma), rinsed sequentially in 1× PBS and distilled water, and air-dried prior to imaging.

H&E Staining. Swiss Webster mice were injected with nano-STATs at 200 U/kg body weight. Mice were sacrificed at the specified time points, and the lungs, heart, spleen, liver, kidney, and brain were isolated and fixed in 4% w/v paraformaldehyde (in 1× PBS) overnight. Fixed organs were paraffin-embedded, sectioned to 5 μm thickness, and H&E stained by the Koch Institute Histology Core.

FPLC Analysis. NanoSTATs were formulated as described above using fluorescently labeled (FITC) heparin (Polysciences). A sample of nanoSTATs was incubated with thrombin (500 nM) at 37 °C for 30 min. Analytical samples of nanoSTATs, nanoSTATs incubated with thrombin, and free heparin were applied to a Superdex 200 column pre-equilibrated with PBS. Absorbance of the column effluent was monitored at a wavelength of 488 nm by a UV flow-through detector.

Alcian Blue Staining. The 25:5:1 PEG:LVPR.RK4:heparin nano-STATs were formulated as described above at a heparin concentration of 3 mg/mL. A 60 μg amount of free heparin or 60 μg of heparin contained in nanoSTATs was loaded into a 1% agarose gel. The gel was run at 60 V in 1× TAE for 20 min, then stained with 0.1% Alcian Blue 8GX (Sigma) in 2% v/v acetic acid. The gel was destained overnight in 2% v/v acetic acid on an orbital shaker prior to imaging on a uniform lightbox.

Azure II Assay. A sample of nanoSTATs was incubated with thrombin at 37 °C for 30 min. NanoSTATs, nanoSTATs incubated with thrombin (500 nM), and free heparin were then mixed with 0.1 mg/mL Azure II solution at a 1:10 volumetric ratio, and the absorbance was read at 530 nm with a SpectraMAX Plus spectrophotometer (Molecular Devices).

aPTT Assay. Varying concentrations of nanoSTATs or free heparin were added to 50 μL of control normal human plasma (Thermo Scientific) and incubated with 50 μL of aPTT reagent (Thermo Scientific) at 37 °C for 3 min. Then 50 μL of 25 mM CaCl$_2$ (Sigma) preincubated at 37 °C was added to samples, and clotting was monitored via absorbance at 605 nm with a SpectraMAX Plus spectrophotometer (Molecular Devices).

Thrombin Generation Assay. Varying concentrations of nano-STATs or free heparin were added to 20 μL of control normal human plasma (Thermo Scientific). Real-time thrombin generation was measured using the Technothrombin TGA kit (Technoclone) using the RD reagent according to manufacturer instructions. The fluorescence was monitored using a TECAN Infinite M200 Pro, and thrombin generation was calculated using the corresponding Excel evaluation software provided by Technoclone.

Circulation Times. Healthy female Swiss Webster mice (3–4 months, n = 3 mice per condition) were injected via tail vein with either nanoSTATs or free heparin at 100 U/kg, formulated with 1× PBS. For measurement of heparin fluorescence, blood samples were collected through retro-orbital blood draw and centrifuged at 2900g for 5 min to isolate plasma, which was then analyzed by fluorimetry using a Spectramax Gemini EM fluorescence microplate reader (Molecular Devices) at excitation/emission wavelengths of 485/538 nm. For measurement of anti-FXa activity, blood samples were collected in tubes containing 3.2% sodium citrate (Sigma) for a final volume ratio of 9:1 (blood:citrate) through retro-orbital blood draws and centrifuged at 2900g for 5 min to isolate the plasma. Heparin activity in the plasma was then determined using the anti-FXa assay.

Tail Bleeding Time Assay. Mice (n = 5–7 per condition) were anesthetized with isoflurane gas and administered nanoSTATs (200 U/kg), free heparin (200 U/kg), or PBS control. After 5 min, 2 mm of distal mouse tail was removed by scalpel. Bleeding time was determined by lightly dabbing the tail with Kimwipe tissues (Kimtech) until bleeding fully ceased for at least 1 min.

Pulmonary Embolism Assay. Bovine fibrinogen (Sigma) was reacted with near-infrared fluorochromes (Vivotag-750-NHS, PerkinElmer) at a 2:1 fluorophore:protein molar ratio in PBS for 1 h and purified by column centrifugation (100 kDa cutoff, Millipore) to remove unreacted fluorophores. Ampules of thromboplastin from rabbit brain (Sigma, #44213) were reconstituted with 2 mL of PBS each. Mice (n = 5 per condition) were anesthetized with isofluorane gas and coadministered nano-STATs (200 U/kg), free heparin (200 U/kg), or PBS control and 1 nmol of VT750-fibrinogen via tail vein injection. After 5 min, mice were injected with thromboplastin (2 uL/g b.w.). After 30 min, mice were euthanized with CO$_2$, and the lungs were harvested and imaged on a LI-COR Odyssey infrared imaging system. Fibrin deposition was then quantified using ImageJ software. For histologic analysis, paraffin-embedded sections of lungs were prepared (Koch Institute Histology Core). Lungs were first fixed by incubating in 4% paraformaldehyde overnight. Hematoxylin and eosin immunochemical staining of lung sections was used to visualize clots in the lungs.

REFERENCES AND NOTES

1. Fink, G. Feedback Actions of Target Hormones on Hypothalamus and Pituitary with Special Reference to Gonadal Steroids. *Annu. Rev. Physiol.* **1979**, *41*, 571–585.
2. Mundy, G. R.; Guise, T. A. Hormonal Control of Calcium Homeostasis. *Clin. Chem.* **1999**, *45*, 1347–1352.
3. Bader, M. Tissue Renin-Angiotensin-Aldosterone Systems: Targets for Pharmacological Therapy. *Annu. Rev. Pharmacol. Toxicol.* **2010**, *50*, 439–465.
4. Lenardo, M.; Chan, K. M.; Hornung, F.; McFarland, H.; Siegel, R.; Wang, J.; Zheng, L. Mature T Lymphocyte Apoptosis—Immune Regulation in a Dynamic and Unpredictable Antigenic Environment. *Annu. Rev. Immunol.* **1999**, *17*, 221–53.
5. Wing, K.; Sakaguchi, S. Regulatory T Cells Exert Checks and Balances on Self Tolerance and Autoimmunity. *Nat. Immunol.* **2010**, *11*, 7–13.
6. Kitano, H. Systems Biology: A Brief Overview. *Science* **2002**, *295*, 1662–1664.
7. Sprinzak, D.; Elowitz, M. B. Reconstruction of Genetic Circuits. *Nature* **2005**, *438*, 443–448.
8. Maitz, M. F.; Freudenberg, U.; Tsurkan, M. V.; Fischer, M.; Beyrich, T.; Werner, C. Bio-Responsive Polymer Hydrogels Homeostatically Regulate Blood Coagulation. *Nat. Commun.* **2013**, *4*.
9. Mackman, N. Triggers, Targets and Treatments for Thrombosis. *Nature* **2008**, *451*, 914–918.
10. Moscucci, M. Frequency and Costs of Ischemic and Bleeding Complications after Percutaneous Coronary Interventions: Rationale for New Antithrombotic Agents. *J. Invasive Cardiol.* **2002**, *14* (Suppl B), 55B–64B.
11. Mannucci, P. M.; Franchini, M. Old and New Anticoagulant Drugs: A Minireview. *Ann. Med.* **2011**, *43*, 116–123.
12. Eikelboom, J. W.; Hirsh, J. Monitoring Unfractionated Heparin with the APTT: Time for a Fresh Look. *Thromb. Haemostasis* **2006**, *96*, 547–552.
13. Ferrari, M. Cancer Nanotechnology: Opportunities and Challenges. *Nat. Rev. Cancer* **2005**, *5*, 161–171.
14. Davis, M. E.; Chen, Z.; Shin, D. M. Nanoparticle Therapeutics: An Emerging Treatment Modality for Cancer. *Nat. Rev. Drug Discovery* **2008**, *7*, 771–782.
15. Sarikaya, M.; Tamerler, C.; Jen, A. K. Y.; Schulten, K.; Baneyx, F. Molecular Biomimetics: Nanotechnology through Biology. *Nat. Mater.* **2003**, *2*, 577–585.
16. von Maltzahn, G.; Park, J.-H.; Lin, K. Y.; Singh, N.; Schwöppe, C.; Mesters, R.; Berdel, W. E.; Ruoslahti, E.; Sailor, M. J.; Bhatia, S. N. Nanoparticles That Communicate *in Vivo* to Amplify Tumour Targeting. *Nat. Mater.* **2011**, *10*, 545–552.
17. Simberg, D.; Duza, T.; Park, J. H.; Essler, M.; Pilch, J.; Zhang, L.; Derfus, A. M.; Yang, M.; Hoffman, R. M.; Bhatia, S.; *et al.* Biomimetic Amplification of Nanoparticle Homing to Tumors. *Proc. Natl. Acad. Sci. U.S.A.* **2007**, *104*, 932–936.
18. Vasudev, S. C.; Chandy, T.; Sharma, C. P. Development of Chitosan/Polyethylene Vinyl Acetate Co-Matrix: Controlled Release of Aspirin-Heparin for Preventing Cardiovascular Thrombosis. *Biomaterials* **1997**, *18*, 375–381.
19. Gutowska, A.; Bae, Y. H.; Jacobs, H.; Mohammad, F.; Mix, D.; Feijen, J.; Kim, S. W. Heparin Release from Thermosensitive Polymer Coatings: *In Vivo* Studies. *J. Biomed. Mater. Res.* **1995**, *29*, 811–821.
20. Baldwin, A. D.; Robinson, K. G.; Militar, J. L.; Derby, C. D.; Kiick, K. L.; Akins, R. E. *In Situ* Crosslinkable Heparin-Containing Poly(Ethylene Glycol) Hydrogels for Sustained Anticoagulant Release. *J. Biomed. Mater. Res., Part A* **2012**, *100A*, 2106–2118.
21. Shiang, Y.-C.; Hsu, C.-L.; Huang, C.-C.; Chang, H.-T. Gold Nanoparticles Presenting Hybridized Self-Assembled Aptamers That Exhibit Enhanced Inhibition of Thrombin. *Angew. Chem., Int. Ed.* **2011**, *50*, 7660–7665.
22. Peters, D.; Kastantin, M.; Kotamraju, V. R.; Karmali, P. P.; Gujraty, K.; Tirrell, M.; Ruoslahti, E. Targeting Atherosclerosis by Using Modular, Multifunctional Micelles. *Proc. Natl. Acad. Sci. U.S.A.* **2009**, *106*, 9815–9819.
23. Jiao, Y.; Ubrich, N.; Marchand-Arvier, M.; Vigneron, C.; Hoffman, M.; Lecompte, T.; Maincent, P. *In Vitro* and *in Vivo* Evaluation of Oral Heparin-Loaded Polymeric Nanoparticles in Rabbits. *Circulation* **2002**, *105*, 230–235.
24. McLean, J. The Thromboplastic Action of Cephalin. *Am. J. Physiol.* **1916**, *41*, 250–257.
25. Hirsh, J.; Warkentin, T. E.; Shaughnessy, S. G.; Anand, S. S.; Halperin, J. L.; Raschke, R.; Granger, C.; Ohman, E. M.; Dalen, J. E. Heparin and Low-Molecular-Weight Heparin Mechanisms of Action, Pharmacokinetics, Dosing, Monitoring, Efficacy, and Safety. *Chest* **2001**, *119*, 64S–94S.
26. Chaikof, E. L. The Development of Prosthetic Heart Valves—Lessons in Form and Function. *N. Engl. J. Med.* **2007**, *357*, 1368–1371.
27. Cronin, R. E.; Reilly, R. F. Unfractionated Heparin for Hemodialysis: Still the Best Option. *Semin. Dial.* **2010**, *23*, 510–515.
28. Capila, I.; Linhardt, R. J. Heparin−Protein Interactions. *Angew. Chem., Int. Ed.* **2002**, *41*, 390–412.
29. Wieduwild, R.; Tsurkan, M.; Chwalek, K.; Murawala, P.; Nowak, M.; Freudenberg, U.; Neinhuis, C.; Werner, C.; Zhang, Y. Minimal Peptide Motif for Non-Covalent Peptide−Heparin Hydrogels. *J. Am. Chem. Soc.* **2013**, *135*, 2919–2922.
30. DeLucia, A., 3rd; Wakefield, T. W.; Andrews, P. C.; Nichol, B. J.; Kadell, A. M.; Wrobleski, S. K.; Downing, L. J.; Stanley, J. C. Efficacy and Toxicity of Differently Charged Polycationic Protamine-Like Peptides for Heparin Anticoagulation Reversal. *J. Vasc. Surg.* **1993**, *18*, 49–58discussion 58−60.
31. Jenny, R. J.; Mann, K. G.; Lundblad, R. L. A Critical Review of the Methods for Cleavage of Fusion Proteins with Thrombin and Factor Xa. *Protein Expr. Purif.* **2003**, *31*, 1–11.
32. Li, S.-D.; Huang, L. Pharmacokinetics and Biodistribution of Nanoparticles. *Mol. Pharmaceutics* **2008**, *5*, 496–504.
33. Petros, R. A.; DeSimone, J. M. Strategies in the Design of Nanoparticles for Therapeutic Applications. *Nat. Rev. Drug Discovery* **2010**, *9*, 615–627.
34. Fischer, D.; Li, Y.; Ahlemeyer, B.; Krieglstein, J.; Kissel, T. *In Vitro* Cytotoxicity Testing of Polycations: Influence of

Polymer Structure on Cell Viability and Hemolysis. *Biomaterials* **2003**, *24*, 1121–1131.

35. Rimann, M.; Luhmann, T.; Textor, M.; Guerino, B.; Ogier, J.; Hall, H. Characterization of Pll-G-Peg-DNA Nanoparticles for the Delivery of Therapeutic DNA. *Bioconjugate Chem.* **2008**, *19*, 548–557.

36. Raschke, R. A.; Reilly, B. M.; Guidry, J. R.; Fontana, J. R.; Srinivas, S. The Weight-Based Heparin Dosing Nomogram Compared with a Standard Care Nomogram: A Randomized Controlled Trial. *Ann. Int. Med.* **1993**, *119*, 874–881.

37. Davie, E. W.; Kulman, J. D. An Overview of the Structure and Function of Thrombin. *Semin. Thromb. Hemost.* **2006**, *32*, 003–015.

38. Mann, K. G.; Butenas, S.; Brummel, K. The Dynamics of Thrombin Formation. *Arterioscler. Thromb. Vasc. Biol.* **2003**, *23*, 17–25.

39. Granger, C. B.; Hirsh, J.; Califf, R. M.; Col, J.; White, H. D.; Betriu, A.; Woodlief, L. H.; Lee, K. L.; Bovill, E. G.; Simes, R. J.; *et al.* Activated Partial Thromboplastin Time and Outcome after Thrombolytic Therapy for Acute Myocardial Infarction: Results from the Gusto-I Trial. *Circulation* **1996**, *93*, 870–878.

40. Anand, S. S.; Yusuf, S.; Pogue, J.; Ginsberg, J. S.; Hirsh, J. Relationship of Activated Partial Thromboplastin Time to Coronary Events and Bleeding in Patients with Acute Coronary Syndromes Who Receive Heparin. *Circulation* **2003**, *107*, 2884–2888.

41. Hemker, H. C.; Giesen, P.; AlDieri, R.; Regnault, V.; de Smed, E.; Wagenvoord, R.; Lecompte, T.; Beguin, S. The Calibrated Automated Thrombogram (CAT): A Universal Routine Test for Hyper- and Hypocoagulability. *Pathophysiol. Haemost. Thromb.* **2002**, *32*, 249–53.

42. Hemker, H. C.; Giesen, P.; Al Dieri, R.; Regnault, V.; de Smedt, E.; Wagenvoord, R.; Lecompte, T.; Béguin, S. Calibrated Automated Thrombin Generation Measurement in Clotting Plasma. *Pathophysiol. Haemostasis Thromb.* **2003**, *33*, 4–15.

43. Hemker, H. C.; Dieri, R. A.; Smedt, E. D.; Béguin, S. Thrombin Generation, a Function Test of the Haemostatic-Thrombotic System. *Thromb. Haemostasis* **2006**, *96*, 553–561.

44. Duchemin, J.; Pan-Petesch, B.; Arnaud, B.; Blouch, M.-T.; Abgrall, J.-F. Influence of Coagulation Factors and Tissue Factor Concentration on the Thrombin Generation Test in Plasma. *Thromb. Haemostasis* **2008**, *99*, 767–773.

45. Passirani, C.; Barratt, G.; Devissaguet, J.-P.; Labarre, D. Long-Circulating Nanopartides Bearing Heparin or Dextran Covalently Bound to Poly(Methyl Methacrylate). *Pharm. Res.* **1998**, *15*, 1046–1050.

46. Brummel, K. E.; Paradis, S. G.; Butenas, S.; Mann, K. G. Thrombin Functions during Tissue Factor−Induced Blood Coagulation. *Blood* **2002**, *100*, 148–152.

47. Comer, M. B.; Cackett, K. S.; Gladwell, S.; Wood, L. M.; Dawson, K. M. Thrombolytic Activity of BB-10153, a Thrombin-Activatable Plasminogen. *J. Thromb. Haemostasis* **2005**, *3*, 146–153.

48. Weiss, E. J.; Hamilton, J. R.; Lease, K. E.; Coughlin, S. R. Protection against Thrombosis in Mice Lacking Par3. *Blood* **2002**, *100*, 3240–3244.

49. Lin, K. Y.; Kwong, G. A.; Warren, A. D.; Wood, D. K.; Bhatia, S. N. Nanoparticles That Sense Thrombin Activity as Synthetic Urinary Biomarkers of Thrombosis. *ACS Nano* **2013**, *7*, 9001–9009.

50. Dawson, K. M.; Cook, A.; Devine, J. M.; Edwards, R. M.; Hunter, M. G.; Raper, R. H.; Roberts, G. Plasminogen Mutants Activated by Thrombin. Potential Thrombus-Selective Thrombolytic Agents. *J. Biol. Chem.* **1994**, *269*, 15989–15992.

51. Korin, N.; Kanapathipillai, M.; Matthews, B. D.; Crescente, M.; Brill, A.; Mammoto, T.; Ghosh, K.; Jurek, S.; Bencherif, S. A.; Bhatta, D.; *et al.* Shear-Activated Nanotherapeutics for Drug Targeting to Obstructed Blood Vessels. *Science* **2012**, *337*, 738–742.

52. Kurz, K. D.; Main, B. W.; Sandusky, G. E. Rat Model of Arterial Thrombosis Induced by Ferric Chloride. *Thromb. Res.* **1990**, *60*, 269–280.

53. Furie, B.; Furie, B. C. Thrombus Formation *in Vivo*. *J. Clin. Invest.* **2005**, *115*, 3355–3362.

54. Arepally, G. M.; Ortel, T. L. Heparin-Induced Thrombocytopenia. *N. Engl. J. Med.* **2006**, *355*, 809–817.

55. Harker, L.; Malpass, T.; Branson, H.; Hessel, E. d.; Slichter, S. Mechanism of Abnormal Bleeding in Patients Undergoing Cardiopulmonary Bypass: Acquired Transient Platelet Dysfunction Associated with Selective Alpha-Granule Release. *Blood* **1980**, *56*, 824–834.

56. LaVan, D. A.; McGuire, T.; Langer, R. Small-Scale Systems for *in Vivo* Drug Delivery. *Nat. Biotechnol.* **2003**, *21*, 1184–1191.

57. Mura, S.; Nicolas, J.; Couvreur, P. Stimuli-Responsive Nanocarriers for Drug Delivery. *Nat. Mater.* **2013**, *12*, 991–1003.

58. Zhao, Y.; Trewyn, B. G.; Slowing, I. I.; Lin, V. S. Y. Mesoporous Silica Nanoparticle-Based Double Drug Delivery System for Glucose-Responsive Controlled Release of Insulin and Cyclic Amp. *J. Am. Chem. Soc.* **2009**, *131*, 8398–8400.

59. Kim, H.; Kang, Y. J.; Kang, S.; Kim, K. T. Monosaccharide-Responsive Release of Insulin from Polymersomes of Polyboroxole Block Copolymers at Neutral pH. *J. Am. Chem. Soc.* **2012**, *134*, 4030–4033.

60. Farmer, T. G., Jr.; Edgar, T. F.; Peppas, N. A. The Future of Open- and Closed-Loop Insulin Delivery Systems. *J. Pharm. Pharmacol.* **2008**, *60*, 1–13.

61. Teien, A. N.; Lie, M.; Abildgaard, U. Assay of Heparin in Plasma Using a Chromogenic Substrate for Activated Factor X. *Thromb. Res.* **1976**, *8*, 413–416.

62. Botnar, R. M.; Perez, A. S.; Witte, S.; Wiethoff, A. J.; Laredo, J.; Hamilton, J.; Quist, W.; Parsons, E. C.; Vaidya, A.; Kolodziej, A.; *et al.* *In Vivo* Molecular Imaging of Acute and Subacute Thrombosis Using a Fibrin-Binding Magnetic Resonance Imaging Contrast Agent. *Circulation* **2004**, *109*, 2023–2029.

63. Hara, T.; Bhayana, B.; Thompson, B.; Kessinger, C. W.; Khatri, A.; McCarthy, J. R.; Weissleder, R.; Lin, C. P.; Tearney, G. J.; Jaffer, F. A. Molecular Imaging of Fibrin Deposition in Deep Vein Thrombosis Using Fibrin-Targeted Near-Infrared Fluorescence. *JACC Cardiovasc. Imaging* **2012**, *5*, 607–615.

64. Gouzy, M. F.; Sperling, C.; Salchert, K.; Pompe, T.; Streller, U.; Uhlmann, P.; Rauwolf, C.; Simon, F.; Bohme, F.; Voit, B.; *et al.* *In Vitro* Blood Compatibility of Polymeric Biomaterials through Covalent Immobilization of an Amidine Derivative. *Biomaterials* **2004**, *25*, 3493–3501.